Reconstruction of 3D Surface Meshes for Blood Flow Simulations of Intracranial Aneurysms

S. Glaßer[1], P. Berg[2], M. Neugebauer[3], B. Preim[1]

[1]*Otto-von-Guericke University of Magdeburg, Department of Simulation and Graphics, Magdeburg, Germany*
[2]*Otto-von-Guericke University of Magdeburg, Department of Fluid Dynamics and Technical Flows, Magdeburg, Germany*
[3]*Fraunhofer Institute MEVIS, Bremen, Germany*

```
contact: sylvia.glasser@ovgu.de
```

Abstract:

The reconstruction of surface meshes of intracranial aneurysms (IA) is the basis for subsequent hemodynamic simulations in order to approximate the internal blood flow. Due to the irregular contrast agent distribution and image artifacts inherent to the medical data acquisition, an initial segmentation of the IA is error-prone and requires several manual correction steps. Within this work, we describe how to create a 3D surface mesh from the medical image data that is well suited for a blood flow simulation via computational fluid dynamic simulation. Our workflow only comprises freely available software tools. We present common artifacts and how to take care of them.

Keywords: Reconstruction, Surface Mesh, Aneurysm, CFD Simulation

1   Problem

Intracranial aneurysms (IA) are pathologic dilatations of the neurovascular vessel wall with a prevalence of approx. 3% [1]. Inherent to IA is the risk of rupture, which may cause a subarachnoid hemorrhage. The treatment options comprise endovascular intervention and neurosurgical clipping with a high rate of complications in relation to the rupture rate of asymptomatic aneurysms. Thus, the rupture rates of small and asymptomatic intracranial aneurysms are reportedly equaled or exceeded by the mortality rate associated with treatment [2]. Therefore, the rupture risk assessment is an important clinical research area.

In clinical practice, the most important rupture risk factors are the type of aneurysm (i.e., asymptomatic or symptomatic), age, sex, and aneurysm size and position [3]. Furthermore, morphological parameters, e.g., irregular shape, orientation, diameter and ratio between aneurysm neck and dome [4], as well as instable and complex blood flow [5, 6] are assumed to be rupture risk factors.

The internal blood flow of IA can be directly measured via phase contrast magnetic resonance imaging (PC-MRI) or approximated via Computational Fluid Dynamics (CFD) simulation. For a successful CFD simulation, i.e., the convergence of the hemodynamic simulation, a volume grid has to be extracted from a high-quality surface mesh representing the vessel geometry [5]. In this work, we present a pipeline that describes how these surface meshes can be acquired from the medical image data. Important aspects are the initial segmentation of the patient-individual aneurysm geometry, the extraction of the 3D surface mesh as well as the optimization of this mesh. Our work is based on the optimization of vascular surface models [7], but it is further optimized and tailored to the extraction of aneurysm surface meshes for CFD simulations. In addition, it only comprises freely available software tools. Since no software tool for the entire and interactive aneurysm surface mesh reconstruction is available, we discuss related work specifically at each step of our pipeline. With the presented work, a large variety of datasets (with 34 IA) were processed, in contrast to the previous work [7], where 7 IA were reconstructed and evaluated for initial experiences.

Image artifacts (e.g., image noise, motion artifacts, cone beam hardening and partial volume effects) induce problems of the surface mesh extraction. An irregular contrast agent accumulation or an insufficient contrast agent flush causes severe problems as well. The contrast agent may not have reached the relevant vessel parts at the acquisition time due to the patient's anatomy and possible pathologies. Furthermore, the complex and pathologic aneurysm geometry itself can hamper the contrast agent flush resulting in a degraded image quality. Further artifacts are so-called *pseudostenoses*. A pseudostenosis is caused by signal superimposition of larger, high-contrast structures (e.g., the aneurysm or its parent vessel) next to smaller vessel parts. Hence, the signal intensities pretend a narrowing at the branching of the smaller vessels. The pseudostenosis is detected by the clinical expert and / or identified in an additional (multimodal) imaging. Finally, blending artifacts arise if two structures (e.g., the aneurysm and a vessel part) are very close to each other. Due to the partial volume effect, a segmentation of all structures comprises an artificial connection of these two structures.
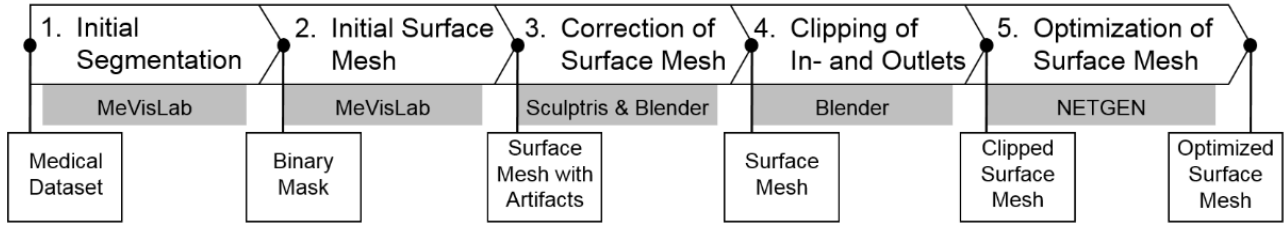
1. Initial Segmentation	2. Initial Surface Mesh	3. Correction of Surface Mesh	4. Clipping of In- and Outlets	5. Optimization of Surface Mesh
MeVisLab	MeVisLab	Sculptris & Blender	Blender	NETGEN
Medical Dataset	Binary Mask	Surface Mesh with Artifacts	Surface Mesh	Clipped Surface Mesh / Optimized Surface Mesh

Fig. 1: Workflow for the extraction of an optimal surface mesh of the aneurysm's geometry for subsequent CFD simulations. The employed software tools are listed in the grey boxes at the bottom of each step.

Our pipeline for the reconstruction, artifact removal, and optimization of the surface mesh, is presented in Fig. 1. The workflow comprises the following steps that will be explained in more detail in the next sections:

1. From the medical image data (see Section 2.1), an initial segmentation of the aneurysm and its connected vessels (see Section 2.2.) is extracted, yielding a voxelized binary mask.
2. The initial segmentation is converted into a surface mesh, i.e., a triangle mesh (see Section 2.3.1).
3. Artifacts of the surface mesh are corrected (see Section 2.3.2).
4. The in- and outlets of the vessels are clipped perpendicular to their centerlines, which is required by the CFD simulation (see Section 2.3.3).
5. The corrected and clipped surface mesh is optimized for an improved mesh quality and the volume grid generation for the CFD simulation (see Section 2.3.4).

2 Material and Methods

In this section, we describe the medical image data and the initial segmentation of the aneurysm model. Afterwards, all steps for the reconstruction of the surface mesh are presented.

2.1. Medical Image Data

The 3D surface mesh is generated from a medical 3D dataset, e.g., a tomographic image dataset. Hence, usually MRI or computer tomography (CT) is employed for image acquisition. In addition, a 3D rotational subtraction angiography (3D RSA) can be acquired with a Dyna CT system. The contrast enhancement of vessels is achieved via contrast agent administration (yielding MR Angiography (MRA) and CT Angiography (CTA) datasets) or the time-of-flight (ToF) MR sequence. The typical extent of the tomographic image data is 512x512x256 voxels. The spatial resolution depends on the imaging modality and varies between ~0.2 - 0.5 mm in the image plane with a slice distance of ~ 0.25 – 0.5 mm. At the moment, 34 surface meshes have been reconstructed with the presented pipeline.

2.2. Initial Segmentation of the Aneurysm

The initial segmentation comprising the aneurysm and connected vessels is extracted from the tomographic image data. Due to the attenuation of the vessels via contrast agent accumulation or MRI ToF imaging, there is a sufficient signal contrast between the lumen of the vessels and the surrounding tissue. Therefore, primitive threshold-based techniques (e.g., *thresholding* or *region growing*) can be applied for the initial segmentation (see Fig. 2). This step of the pipeline is realized using MeVisLab 2.6.2 (MeVis Medical Solutions AG, Bremen, Deutschland, www.mevislab.de), a freely available software tool with dedicated methods for the medical image processing and visualization. Hence, our pipeline comprises the straightforward segmentation via *thresholding*. Thus, image artifacts lead to artifacts of the resulting surface mesh and are corrected later on (see Section 2.3.1). In contrast to this procedure, also complex segmentation approaches can be employed, e.g., model-based approaches for 3D RSA datasets [8]. To extract surface meshes for aneurysms with low contrast next to the high contrast enhanced major vessels, multi-range filters were employed [9]. Furthermore, *level sets* were adapted for the segmentation of IA [10,11]. Semi-automatic methods require specific user input to avoid an over- or undersegmentation, e.g., the user can steer the segmentation method via multiple placement of seeding points [12]. Geometrical presentations of vessels can be extracted via model-based approaches, where artifacts are reduced due to the model assumptions [13]. In contrast, our pipeline comprises artifact correction in a post-processing step (see Section 2.3.1). However, the model-based segmentation often requires circular or elliptical vessel cross-sections, whereas IA often exhibit irregular vessel shapes and strongly varying vessel cross-sections. Therefore, we chose the thresholding approach and subsequent artifact correction.
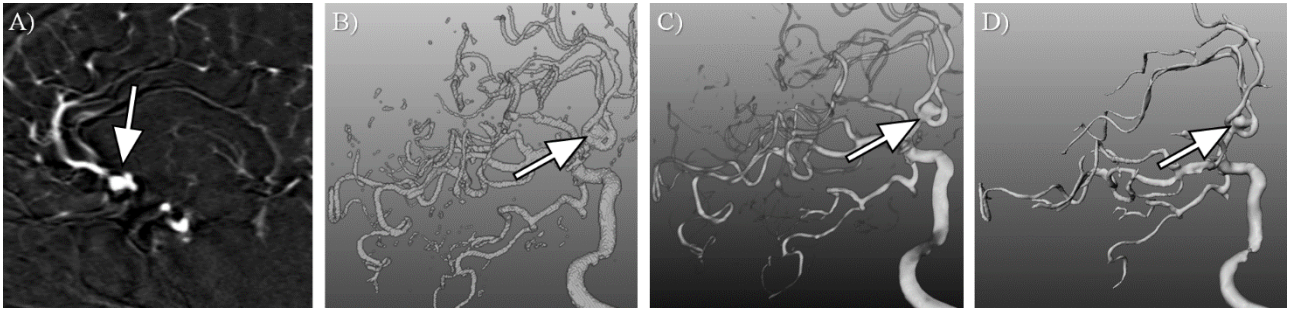
Fig. 2: A) Slice image of a 3D RSA dataset with an aneurysm (see arrow). B) shows a direct volume rendering view with primitive windowing. C) presents the 3D view of the binary mask extracted with *thresholding*. The surface mesh depicted in D) was extracted via *marching cubes* applied to the binary mask. All views were generated with MeVisLab.

2. 3. Extraction of the Surface Mesh

2.3.1. Geometrical Representation

For the generation of the geometrical representation required for volume grid generation and CFD simulation, the previously described initial segmentation is converted. We apply the *marching cubes* algorithm (available in MeVisLab) to the binary mask. The extracted surface mesh is a triangle mesh of poor quality, i.e., it contains acute-angled triangles or artifacts like sharp edges or small bumps due to the voxelized initial segmentation mask. These problems have to be corrected for a successful subsequent CFD simulation. However, irregular pathologies are contained in the initial surface mesh due to the straightforward approach. The initial surface mesh is smoothed with a Laplacian kernel (available in MeVisLab). Naturally, for the generation of surface meshes from a binary mask, other methods are employed as well, for example implicit methods like the *MPU implicits* approach [14]. However, the result of such implicit methods depends on the quality of the initial segmentation (recall Section 2.2). Since our pipeline comprises a primitive segmentation (i.e., *thresholding*) followed by the correction and reduction of artifacts afterwards, we focus on explicit methods like the *marching cubes* technique.

2.3.2. Manual Correction of Artifacts

As described in the previous paragraph, a global smoothing is applied to the initial surface mesh (carried out in MeVisLab). In the next step, we focus on the local correction of artifacts. We use Sculptris 1.02 (Pixologic, http://pixologic.com/sculptris/), a free software tool for 3D modeling based on surface meshes.
Our workflow comprises the correction of two types of local artifacts:

- Small artifacts like bumps or valley of the mesh and pseudostenoses.
- Blending artifacts at two close vessel parts.

We locally smooth small bumps or valleys, i.e., artifacts which are not small vessels, see Fig. 3. A pseudostenosis is removed by thickening of the affected vessel parts. Sculptris provides the option to locally adjust a *region of interest* (ROI). A circle-shaped ROI is projected on the surface mesh (recall Fig. 3C) and all actions only affect triangles within this ROI. The user can interactively and intuitively change the size of the ROI and its position.
Blending artifacts may arise if two contrast-enhanced structures are very close to each other (recall Section 1). The correction involves two steps. First, the blending is removed with Blender 2.74 (Blender Foundation, Amsterdam, the Netherlands, https://www.blender.org/), an open-source 3D modeling, graphics and animation program. To avoid holes in the surface mesh, we create a closed cube mesh. We rescale the cube and position it such that it encloses the blending area. Next, we carry out Boolean operations, i.e., we subtract the cube mesh from the aneurysm surface mesh yielding a surface mesh without the blending, see Fig. 4. Afterwards, the planar and cropped areas are smoothed with Sculptris.
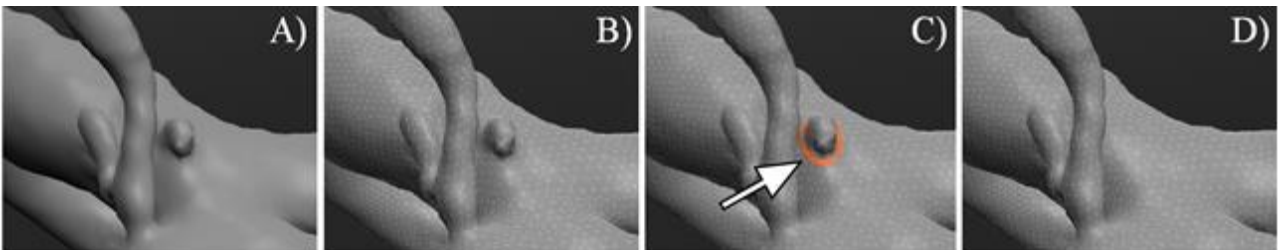

Fig. 3: Correction of small artifacts with Sculptris (A-D). The triangles forming the artifact were locally (see arrow and the orange highlighting of the ROI) smoothed and merged.
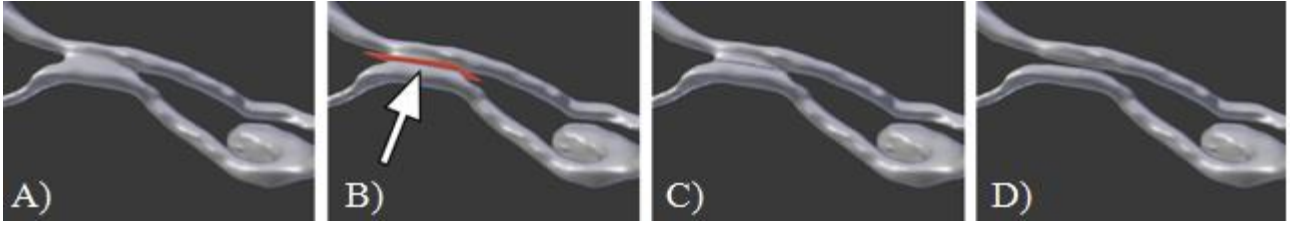
Fig. 4: Correction of a blending artifact (A-D). A quad is added to the 3D scene in Blender (see arrow in B) and cut with the surface mesh via Boolean difference operation (C). The surface mesh was locally smoothed with Sculptris (D).

2.3.3. Generation of Inlets and Outlets

Another prerequisite for the CFD simulation is the correct definition of the inlet and outlets. The CFD simulation requires assignments to these cross-sections, e.g., an inlet curve representing the incoming blood flow velocity or the resistance of the blood flow through the outlets. In general, these conditions need to be defined perpendicular to the direction of the blood flow. Thus, we have to create faces for the inlets and outlets perpendicular to the vessel centerline. Therefore, we employ a cutting of the surface mesh using Blender again, see Fig. 5. The example shows a bended vessel with a cube added to the 3D scene. It was placed such that the resulting cutting plane is perpendicular to the centerline. Next, the cutting is carried out via the Boolean difference operator in Blender. To provide a sufficiently long enough and straight vessel section for the CFD simulation, the newly created cutting plane is extruded by at least six mean vessel diameters. This enables the development of a complete flow profile (e.g., a parabolic flow profile) and reduces the influence of boundary conditions, before the simulated blood enters the patient-specific geometry during the simulation.
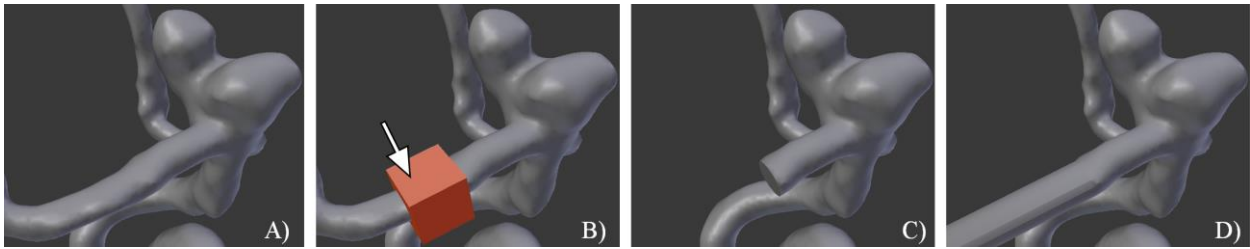

Fig. 5: Illustration of the cutting of an outlet cross-section. A cube is added to the 3D scene (see arrow in B), which cuts the surface mesh using Boolean difference operations (C). The newly created cutting plane is extruded in order to maintain optimal CFD inflow conditions.

2.3.4 Optimization of the Surface Mesh

Finally, the optimization of the surface mesh is carried out to improve the triangle quality, i.e., improved triangle edge ratio and homogeneous triangle size. The resulting optimized surface mesh is the prerequisite for a successful volume grid generation and for the stability and convergence of the CFD simulation, respectively. For the optimization, we employ NETGEN 5.0 (an open source program, http://sourceforge.net/projects/netgen-mesher/, [15]), which uses an advancing front method. Hence, mesh optimization algorithms as well as a hierarchical remeshing are included. The user can define feature edges, which are preserved during the remeshing. We select the edges of the in- and outlets, a process that is semi-automatically carried out by defining the desired minimum angle between two adjacent triangles (edges with two adjacent triangles fulfilling this requirement are defined as feature edge). After the optimization, the feature edges of the inlets and outlets are preserved and the triangle quality has been improved (see Fig. 6). Now, the resulting surface mesh is ready for the volume grid generation and the subsequent CFD simulation. Alternatively, also commercial tools, e.g., INRIA's YAMS [16], are employed for the aneurysm surface mesh optimization [17].
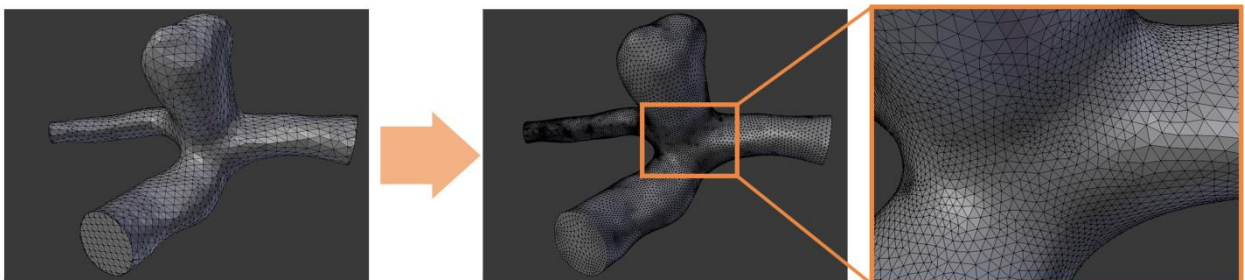

Fig. 6: Optimization of the initial surface mesh (left) via NETGEN yields homogeneously sized triangles and an improved triangle edge ratio. Furthermore, the triangle size is adapted to the curvature of the surface (see inlet).

3   Results

With the presented pipeline, optimized surface meshes are generated. Afterwards, the surface mesh is compared to the original medical data by a medical expert using a comparative visualization realized by MeVisLab, see Fig. 7. The original dataset is depicted with a rendering based on a windowing transfer function. The extracted surface mesh is highlighted with indirect surface visualization (both techniques are available in MeVisLab). The quality of the surface mesh topology is mainly influenced by the artifacts listed in Section 1. Often, the comparative visualization confirms sufficient quality of the surface mesh (i.e., no part is missing, artifacts are corrected). In case the original image data strongly differs from the extracted mesh, irregular contrast agent distributions have to be identified and, if necessary, corrected. This examination usually involves a clinical expert to account for an anatomically plausible vessel representation. If the comparative visualization only reveals small differences, like small bumps or local over- and under-segmentations, the errors are corrected with Sculptris and the surface mesh is reloaded.

Fig. 7: Comparative visualization with MeVisLab. A rendering of the 3D RSA with IA (arrow) is shown on the left. The user can modify the coloring of the surface mesh. In the center, red is assigned to the original dataset and white to the surface mesh. On the right, white is assigned to the original dataset and green to the surface mesh.

4   Discussion

The main drawback of the presented pipeline is the integration of four different software tools: MeVisLab, Sculptris, Blender and NETGEN. Thus, the user has to become familiar with these tools and develop a certain expertise for each of them and the target geometry needs to be exchanged between the different separate tools. Especially for image data with low quality and many correction steps, the surface generation process is very complex and may get tedious. However, only freely available software tools were employed. The post processing, i.e., the manual correction allows for integration of expert knowledge. Hence, also irregularly shaped parts of IA and their parent vessels can be reconstructed.

In summary, a unified solution for segmentation, smoothing, mesh extraction, artifact correction, cutting and optimization seems to be desirable and could help to faster guide the user through this process and support the exchange with the medical experts. However, each software tool has its advantages (including a sophisticated user interface) and it is questionable that all functionalities can be easily transferred into a unified solution.

5   Conclusion

The presented pipeline allows for the extraction of an optimized surface mesh, which can be employed for volume grid generation and subsequent CFD simulation. The workflow was subdivided into the most important parts and explained in more detail. Researchers of the clinical or computational domain can easily adapt this workflow and replace certain steps with their own methods. Also, typical artifacts were discussed and a guidance for correction of these artifacts was provided. For the improved rupture risk assessment, the extraction of additional features beyond attributes related to the CFD simulation can be carried out. For example, the surface mesh can be employed for the extraction of the ostium plane or the automated determination of the distance between aneurysm dome and aneurysm neck including centerline detection or parametric extrusion techniques.

6   Acknowledgements

7 References

[1] S. Juvela, *Prevalence of Aneurysms and Risk Factors for Intracranial Aneurysms*, The Lancet Neurology, **10(7)**, 595 – 597 (2011)

[2] D. O. Wiebers, *Unruptured Intracranial Aneurysms: Natural History, Clinical Outcome, and Risks of Surgical and Endovascular Treatment*, The Lancet, **362(9378)**, 103-110 (2003)

[3] M. J. Wermer, I. C. van der Schaaf, A. Algra, G. J. Rinkel, *Risk of Rupture of Unruptured Intracranial Aneurysms in Relation to Patient and Aneurysm Characteristics: An Updated Meta-Analysis,* Stroke, **38(4)**, 1404-1410 (2007)

[4] R. Lall, C. Eddleman, B. Bendok, H. Batjer, *Unruptured Intracranial Aneurysms and the Assessment of Rupture Risk Based on Anatomical and Morphological Factors: Sifting Through the Sand of Data*, Neurosurgical Focus, **26(5)**, E2 (2009)

[5] J. R. Cebral, M. A. Castro, S. Appanaboyina, C. M. Putman, D. Millan, A. F. Frangi, *Efficient Pipeline for Image-Based Patient-Specific Analysis of Cerebral Aneurysm Hemodynamics: Technique and Sensitivity*, IEEE Transactions on Medical Imaging, **24(4)** 457–467 (2005)

[7] T. Mönch, M. Neugebauer, B. Preim, *Optimization of Vascular Surface Models for Computational Fluid Dynamics and Rapid Protoptyping*, Proc. of Workshop on Digital Engineering, 16-23 (2011)

[6] J. Xiang, S. K. Natarajan, M. Tremmel, D. Ma, J. Mocco, L. N. Hopkins, A. H. Siddiqui, E. I. Levy, H. Meng, *Hemodynamic-Morphologic Discriminants for Intracranial Aneurysm Rupture*, Stroke, **42(1)**, 144-152 (2011)

[8] M. Spiegel, *Specific Cerebral Vessel Segmentation with Application in Hemodynamic Simulation*, PhD Thesis, University of Erlangen, Germany (2011)

[9] M. W. Law, A. C. S. Chung, *Segmentation of Intracranial Vessels and Aneurysms in Phase Contrast Magnetic Resonance Angiography Using Multirange Filters and Local Variances.* IEEE Transactions on Image Processing, **22(3),** 845–859 (2013)

[10] J. R. Cebral, M. Hernandez, A. F. Frangi, C. M. Putman, R. Pergolizzi, J. E. Burgess, *Subject-Specific Modeling of Intracranial Aneurysms,* Proc. of SPIE Medical Imaging, 319-327 (2004)

[11] A. Firouzian, R. Manniesing, Z. Flach, R. Risselada, F. van Kooten, M. Sturkenboom, A. Lugt, W. J. Niessen. *Intracranial Aneurysm segmentation in 3D CT Angiography: Method and Quantitative Validation with and without prior Noise Filtering*, European Journal of Radiology, **79(2)**, 299-304 (2011)

[12] L. Antiga, M. Piccinelli, L. Botti, B. Ene-Iordache, An. Remuzzi, D. A. Steinman, *An Image-Based Modeling Framework for Patient-Specific Computational Hemodynamics*, Medical & Biological Engineering & Computing, **46(11)** 1097-1128 (2008)

[13] M. Hernandez, A. F. Frangi, *Non-Parametric Geodesic Active Regions*: *Method and Evaluation for Cerebral Aneurysm Segmentation in 3DRA and CTA*, Medical Image Analysis, **11(3)**, 224-241 (2007)

[14] C. Schumann, M. Neugebauer, R. Bade, B. Preim, H.-O. Peitgen, *Implicit Vessel Surface Reconstruction for Visualization and Simulation*, Computer Assisted Radiology and Surgery, 2008, **2(5)**, 275-286, (2008).

[15] J. Schöberl, *Netgen-An Advancing Front 2D/3D-Mesh Generator Based on Abstract Rules*, Computing and Visualization in Science, **1**, 41-52 (1997)

[16] P. Frey, *Yams: A Fully Automatic Adaptive Isotropic Surface Remeshing Procedure,* Technical Report RT-0252, pp.36, INRIA, France, (2001)

[17] M. Baoshun, R. E. Harbaugh, M. L. Raghavan, *Three-Dimensional Geometrical Characterization of Cerebral Aneurysms*, Annals of Biomedical Engineering, **32(2)**, 264-273 (2004)